Am J Physiol Lung Cell Mol Physiol
280: L390–L399, 2001.

Cytokine-induced changes in chromatin structure and in vivo footprints in the inducible NOS promoter

JANE K. MELLOTT,[1] HARRY S. NICK,[2] MICHAEL F. WATERS,[1] TIMOTHY R. BILLIAR,[3] DAVID A. GELLER,[3] AND SARAH E. CHESROWN[4]
Departments of [1]Biochemistry and Molecular Biology, [2]Neuroscience, and [4]Pediatrics, University of Florida, Gainesville, Florida 32610; and [3]Department of Surgery, University of Pittsburgh, Pittsburgh, Pennsylvania 15261

Received 17 February 2000; accepted in final form 29 September 2000

Mellott, Jane K., Harry S. Nick, Michael F. Waters, Timothy R. Billiar, David A. Geller, and Sarah E. Chesrown. Cytokine-induced changes in chromatin structure and in vivo footprints in the inducible NOS promoter. *Am J Physiol Lung Cell Mol Physiol* 280: L390–L399, 2001.—Transcription of the human inducible nitric oxide synthase (*iNOS*) gene is regulated by inflammatory cytokines in a tissue-specific manner. To determine whether differences in cytokine-induced mRNA levels between pulmonary epithelial cells (A549) and hepatic biliary epithelial cells (AKN-1) result from different protein or DNA regulatory mechanisms, we identified cytokine-induced changes in DNase I-hypersensitive (HS) sites in 13 kb of the iNOS 5′-flanking region. Data showed both constitutive and inducible HS sites in an overlapping yet cell type-specific pattern. Using in vivo footprinting and ligation-mediated PCR to detect potential DNA or protein interactions, we examined one promoter region near −5 kb containing both constitutive and cytokine-induced HS sites. In both cell types, three in vivo footprints were present in both control and cytokine-treated cells, and each mapped within a constitutive HS site. The remaining footprint appeared only in response to cytokine treatment and mapped to an inducible HS site. These studies, performed on chromatin in situ, identify a portion of the molecular mechanisms regulating transcription of the human *iNOS* gene in both lung- and liver-derived epithelial cells.

nitric oxide synthase; deoxyribonuclease I-hypersensitive sites; inflammatory cytokines; lung epithelial cells; liver epithelial cells

EXPRESSION OF THE HUMAN inducible nitric oxide (NO·) synthase (*iNOS*) gene is dramatically induced by inflammatory cytokines in many tissues including lung and liver epithelia (11, 13, 32). Production of NO· by iNOS is thereby increased during the inflammatory response, adding to the local defense against invading microbes (8, 28) or potentially contributing to free radical-mediated tissue injury in inflammatory disorders affecting these and other organs (3, 15, 16, 33, 39, 40).

Kroncke et al. (19) recently reviewed evidence of iNOS involvement in human diseases and concluded that the functional role of epithelial iNOS activity is not well understood. In lung epithelium, iNOS expression is dramatically increased in patients with asthma, and nitration of proteins in these cells provides evidence of the functional consequences of increased NO· (13). Because corticosteroid treatment of asthmatic patients leads to clinical improvement and decreased levels of exhaled NO·, it is often speculated that epithelial iNOS activity contributes to the pathogenesis of asthma (1, 13). Within the liver, both hepatocytes and biliary lining epithelium show iNOS expression in response to proinflammatory Th1 cytokines. Although iNOS levels are increased in chronic viral hepatitis (24) and cirrhosis (18), the functional significance is unknown. Hepatic regulation and function of iNOS in the liver was recently reviewed by Taylor et al. (35). Based on pharmacological blockade of iNOS, these authors cite the interesting hepatic cytoprotective effect of iNOS expression in sepsis and ischemia-reperfusion.

Cytokines induce *iNOS* expression at the level of transcription, but the specific combination of cytokines leading to a maximal increase in mRNA levels is different among tissues (7, 13). Tissue-specific regulation of human *iNOS* may be important, therefore, in determining its local physiological role and pathophysiological potential. To begin to define those regions of *iNOS* that confer cytokine responsiveness, deletion analyses with the 5′-flanking sequence have been done in liver, lung, and colonic epithelial cell lines (7, 20, 23, 27, 34). Results have shown that compared with the murine *iNOS* promoter, a much larger region of the 5′-flanking sequence of human *iNOS* is required for maximal cytokine induction. More than 3.8 kb of the human *iNOS* 5′-flanking sequence is required for cytokine induction of reporter genes in both liver and colonic cell lines (7, 23). In DLD-1 colonic adenoma-derived cells, Linn et al. (23) showed that sequences between 8.7 and 10.7 kb upstream from the transcription initiation site were necessary for cytokine responsiveness and functioned as a classic enhancer. In contrast, Spitsin et al. (34) reported that sequences between −0.4 and −1.6 kb

Address for reprint requests and other correspondence: S. E. Chesrown, Box 100296 HSC, Dept. of Pediatrics, Univ. of Florida, Gainesville, FL 32610 (E-mail: chesrse@peds.ufl.edu).

The costs of publication of this article were defrayed in part by the payment of page charges. The article must therefore be hereby marked "*advertisement*" in accordance with 18 U.S.C. Section 1734 solely to indicate this fact.

supported modest twofold cytokine responsiveness in the A549 lung epithelial adenocarcinoma cell line, whereas Nunokawa et al. (27) showed that 3.2 kb of the *iNOS* 5′-flanking sequence supported a threefold increase in reporter gene expression in these same cells. These data suggest interesting and important tissue-specific differences in human *iNOS* regulation at the transcriptional level.

In addition to deletion analysis, large regions of chromatin can be screened for potential regulatory regions with DNase I-hypersensitive (HS) site analysis. Local changes in chromatin structure accompany the activation of gene transcription through the binding of *trans*-acting protein factors to DNA response elements (12). To localize regulatory sites within 13 kb of the 5′-flanking region of human *iNOS*, permeabilized control and cytokine-treated cells were exposed to increasing concentrations of DNase I to probe the chromatin structure. In both the A549 human pulmonary adenocarcinoma cell line and the AKN-1 biliary epithelial cell line, we compared DNase I-digested chromatin isolated from control cells and cells treated with a combination of interleukin (IL)-1β, tumor necrosis factor (TNF)-α, and interferon (IFN)-γ. The results identified both unique and overlapping constitutive and cytokine-induced HS sites in these cell types extending from the transcriptional start site to −12 kb.

Using the locations of DNase I HS sites as a guide, we performed dimethyl sulfate (DMS) ligation-mediated (LM) PCR in vivo footprint analysis to identify potential DNA binding sites of regulatory proteins at single-nucleotide resolution. The data identified three constitutive and two cytokine-induced binding sites on guanine residues between −5 and −5.5 kb in the human *iNOS* 5′-flanking sequence from both cell types.

EXPERIMENTAL PROCEDURES

Cell culture. A549 cells, a human pulmonary epithelial-like cell line originally isolated from a lung adenocarcinoma (22), were cultured in 90% Ham's F-12K medium (Sigma, St. Louis, MO) and 10% fetal bovine serum supplemented with 10 mM L-glutamine and an antibiotic-antimycotic solution (Sigma). AKN-1 cells, a hepatic biliary epithelial cell line isolated by serial dilution from a normal human liver (7, 29), were cultured in serum-free, chemically defined medium as previously described (7). To induce *iNOS*, eight 10-cm tissue culture dishes of 90% confluent A549 or AKN-1 cells were incubated in serum-free Ham's F-12K medium or serum- and dexamethasone-free medium for 8 h in the presence of 100 U/ml of recombinant human (rh) IL-1β (National Cancer Institute), 500 U/ml of rhTNF-α (Genentech), and 250 U/ml of rhIFN-γ (Genentech). Control cells were incubated in serum- and dexamethasone-free medium without the cytokines. RNA isolation and Northern analysis were performed as previously described (38).

Cell permeabilization. Control and treated cells were trypsinized and pooled in separate centrifuge tubes and then washed in 30 ml of medium with serum. The cells were pelleted at 1,500 rpm for 5 min at 4°C and then gently resuspended in 10 ml of ice-cold *solution A* (150 mM sucrose, 80 mM KCl, 35 mM HEPES, pH 7.4, 5 mM K_2HPO_4, 5 mM $MgCl_2$, and 0.5 mM $CaCl_2$) (31). After recentrifugation, the pellets were resuspended in 4.0 ml of ice-cold *solution A*. The cells were permeabilized with 4.0 ml of room temperature 0.1% lysophosphatidylcholine (Calbiochem) in *solution A*, triturated, incubated on ice for ~2 min, and diluted to 40 ml with ice-cold *solution A*. Permeabilized cells were centrifuged at 1,800 rpm for 5 min at 4°C. The pellets were resuspended in 3 ml of ice-cold *solution A* and placed on ice before immediate DNase I digestion.

DNase I digestion and genomic DNA isolation. Duplicate sets of tubes containing increasing amounts (range 0–36 U/ml) of DNase I (Worthington Biochemical) were prepared on ice. Three hundred microliters of a permeabilized cell suspension from control or treated samples were added, gently mixed, and incubated for 4 min in a 37°C water bath. The cells were lysed by the addition of 300 μl of freshly prepared DNA lysis buffer (4% SDS, 0.2 M EDTA, and 800 μg/ml of proteinase K). DNase I-digested genomic DNA was purified by sequential organic extraction followed by RNase digestion and ethanol precipitation. Genomic DNA was resuspended to a final concentration of ~1 μg/μl in 1× Tris-EDTA (TE). To ensure that DNase I digestion had occurred, all samples were size fractionated and stained with ethidium bromide. Loss of high molecular weight DNA and the appearance of a continuous gradient of smaller molecular weight DNA was evidence of DNase I cleavage.

Southern analysis. Fifteen micrograms of DNase I-cleaved DNA from control and cytokine-induced cells were digested with an appropriate restriction enzyme and size fractionated on either 0.8% high gelling temperature agarose (FMC) or 2.5% NuSieve 3:1 (FMC) gels overnight at 40 V. The gels were washed, and DNA was electrotransferred to Hybond N+ nylon membranes (Amersham).

Double-strand fragments of ~400 bp were obtained by either restriction digestion of the human *iNOS* promoter and cDNA constructs or by PCR amplification with gene-specific primers. Probes were verified to be single copy and to hybridize to restriction fragments of the predicted sizes by Southern hybridization to both human genomic DNA and cosmid *iNOS* constructs. Single-copy probe fragments were radiolabeled by random-hexamer primer extension with [α-^{32}P]dATP and a random-primer DNA labeling kit (Life Technologies). Hybridization and washing were done as previously described (38) followed by autoradiography. The HS site analysis was reproduced in four independent experiments.

In vivo and in vitro DMS treatment. A549 and AKN-1 cells were incubated for 8 h with and without rhIL1-β, rhTNF-α, and rhIFN-γ as described in *Cell culture*. After a wash with room temperature PBS, the cells were incubated with 20 ml of room temperature PBS containing 0.5% DMS for 1 min. The DMS reaction was terminated, and the cells were lysed with 10 ml of DNA lysis buffer (50.0 mM Tris·HCl, pH 8.5, 50 mM NaCl, 25 mM EDTA, pH 8.0, 0.5% SDS, and 300 μg/ml of proteinase K) and incubated overnight at room temperature. The DMS-treated genomic DNA was purified by organic extraction, RNase digestion, and ethanol precipitation. After purification, DMS-treated DNA was dissolved in double-distilled water and cleaved with piperidine as described below (17).

Human genomic DNA previously isolated and purified of proteins was treated in vitro with DMS and served as a control to show all guanine residues in the area of interest. Purified DNA was digested with *Eco*RI at 37°C for 1 h and purified by organic extraction and ethanol precipitation. DNA was resuspended in 10 μl of sterile double-distilled H_2O and 400 μl of 50 mM sodium cacodylate, pH 8.0, and 1 mM EDTA. To this solution, 0.25 μl of DMS was added and incubated for 20 s. The DMS reaction was stopped by the addition of 50 μl of ice-cold stop buffer (1.5 M sodium acetate,

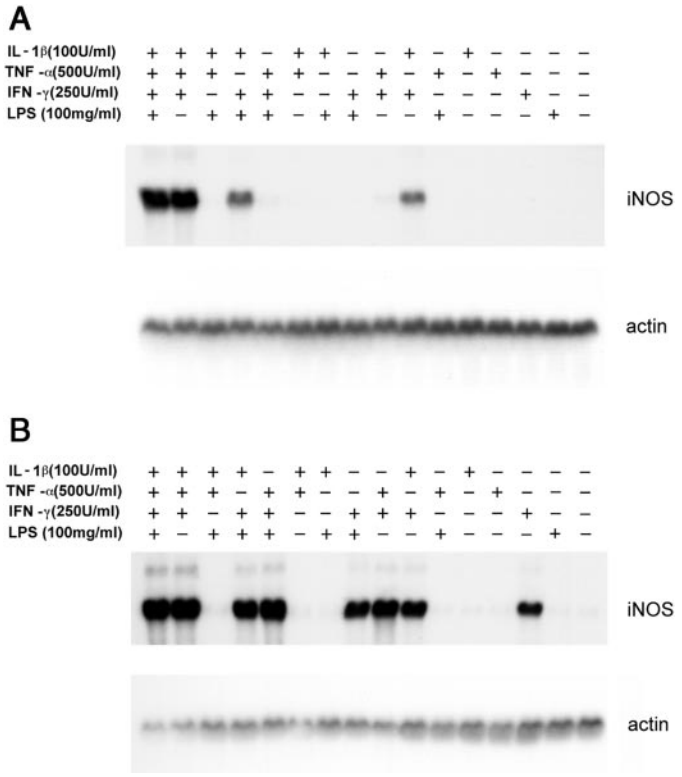

Fig. 1. Northern analysis of cells stimulated with all possible combinations of interleukin (IL)-1β, tumor necrosis factor (TNF)-α, interferon (IFN)-γ, and lipopolysaccharide (LPS). A549 (*A*) and AKN-1 (*B*) cells were grown to confluence and stimulated for 8 h with the inflammatory mediators as indicated. RNA was then harvested and subjected to Northern analysis. iNOS, inducible nitric oxide synthase. +, Presence of the mediator; −, absence of the mediator.

pH 7.0, and 100 μg/ml of tRNA) and 750 μl of ice-cold ethanol. Samples were frozen in a dry ice-ethanol bath and precipitated at 13,000 rpm for 30 min at 4°C. The DNA was resuspended in 250 μl of 0.3 M sodium acetate, precipitated, and washed in 95% ethanol. The vacuum-dried pellet was resuspended in double-distilled H_2O before piperidine cleavage. DMS-treated DNA was heated to 95°C for 30 min in 200 μl of 1 M piperidine, precipitated as described by Kuo et al. (19a), and resuspended in 100 μl of 1× TE. Piperidine was completely removed by drying in a vacuum concentrator, and the pellets were rediluted to 1 μg/μl in 1× TE (17). All in vivo footprinting data were reproduced in three independent experiments.

Ligation-mediated PCR. Piperidine-cleaved DMS-treated DNA samples and primers were amplified for 1 cycle at 95°C for 3.5 min, 65°C for 30 s, and 76°C for 3 min, then for 19 cycles at 95°C for 30 s, 65°C for 30 s, and 76°C for 3.0 min + 5 s/cycle for each of the 19 cycles, and finally for 1 cycle at 95°C for 30 s, 65°C for 30 s, and 76°C for 10 min. See Figs. 5 and 6 for a description of the respective primers.

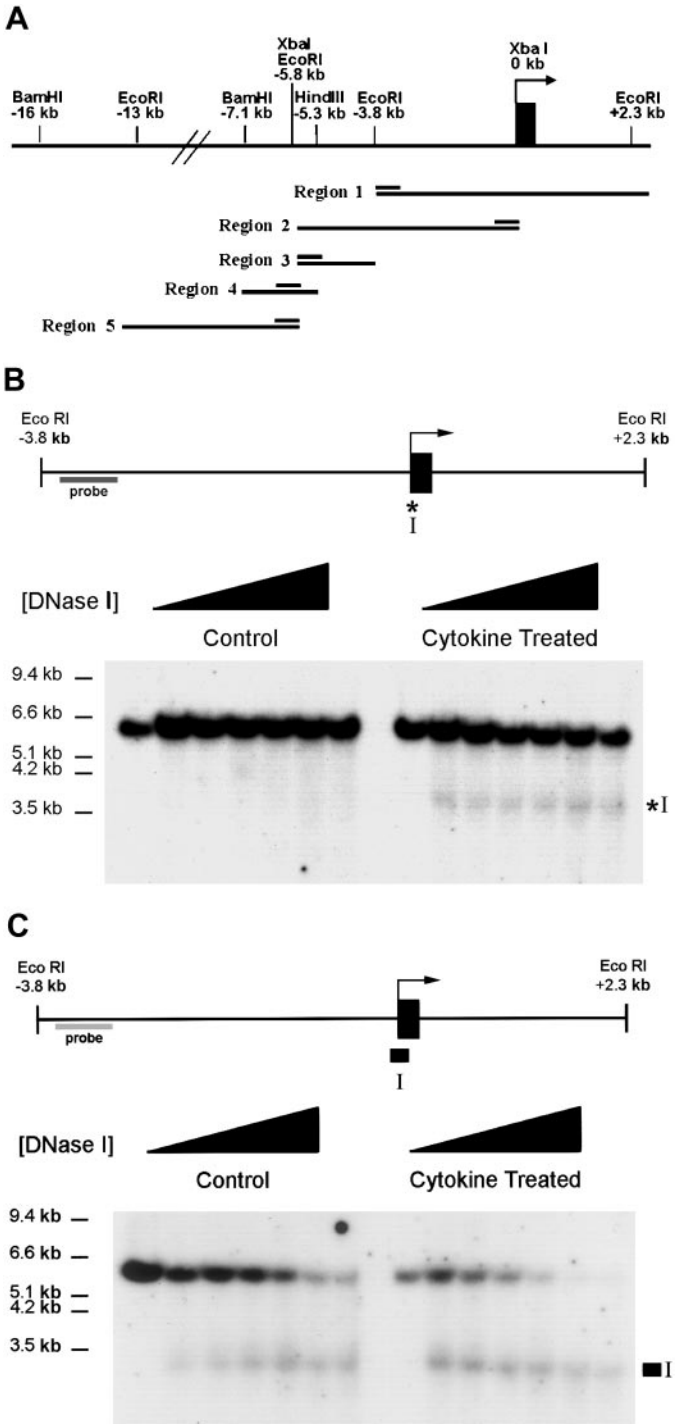

Fig. 2. Chromatin structure analysis of human *iNOS*. *A*: restriction fragments and single-copy hybridization probes (*regions 1–5*) used to map DNase I-hypersensitive (HS) sites are illustrated below a restriction map of the *iNOS* promoter region. Arrow, transcription start site over the 1st exon. *B*: A549 cells were grown to confluence and either treated for 8 h with IL-1β, TNF-α, and IFN-γ or kept as control, unstimulated samples. After induction, the samples were permeabilized with lysophosphatidylcholine and digested with DNase I as described in EXPERIMENTAL PROCEDURES. After purification, the samples were digested with *Eco*RI and DNase I-HS sites were detected by Southern analysis. *Top*: analysis of *region 1* in the promoter. The hybridization probe was a 500-bp fragment that abutted the *Eco*RI site at −3.8 kb. Control samples were not induced with cytokines. *Bottom*: samples that were digested in situ with increasing amounts of DNase I ([DNase I]). *Lane 1* in each group received no DNase I digestion, and only the intact restriction fragment hybridized to the probe. *, Position of the inducible DNase I-HS site. *C*: AKN-1 cells treated as in *B*. Solid box, position of the constitutive HS site that was present in both control and cytokine-treated cells.

To resolve the sequencing ladder, the samples were size fractionated in 5% LongRanger acrylamide (FMC) in 50 mM Tris-borate-EDTA at 90 W. The gel was electrotransferred to Hybond N+ nylon membrane (Amersham), prehybridized at 45°C for 15 min in hybridization buffer (0.5 M sodium phosphate, pH 7.2, 7% SDS, 1% BSA, and 1 mM EDTA) followed by overnight hybridization with a ^{32}P end-labeled gene-specific oligonucleotide at 45°C.

A computer analysis of the sequence surrounding the inducible and constitutive footprints was carried out with TFSEARCH (http://pdap1.trc.rwcp.or.jp/research/db/TFSEARCH.html) with all matrices and an 85.0 threshold score and with MatInspector version 2.2 (http://transfac.gbf.de/cgi-bin/matSearch/matsearch.pl) with all matrices, a core similarity of 0.80, and a matrix similarity equal to 0.85.

RESULTS

Human *iNOS* is regulated primarily at the level of transcription, and its mRNA is often undetectable in cells that have not been stimulated with proinflammatory mediators (26). In contrast to murine iNOS that is induced by a single cytokine or lipopolysaccharide (LPS), various combinations of cytokines are necessary to maximally induce human *iNOS* mRNA (5, 6, 11). We therefore determined the precise combinations of cytokines necessary for the induction of human *iNOS* steady-state mRNA levels in A549 and AKN-1 cells. Figure 1 shows a Northern analysis of both A549 and AKN-1 cells stimulated with all possible combinations of the cytokines IL1-β, IFN-γ, and TNF-α and bacterial LPS. Maximal induction in A549 cells (Fig. 1*A*) required treatment with a combination of all three cytokines, whereas the addition of LPS, a potent inducing agent of murine *iNOS*, had no detectable effect. Both IL-1β and IFN-γ were necessary to minimally induce message levels in the A549 cells. In AKN-1 cells (Fig. 1*B*), maximal induction also required the addition of all three cytokines. However, IFN-γ alone was sufficient to induce *iNOS* expression in the AKN-1 cells. Because these two epithelial cell lines have different requirements for cytokines to minimally induce *iNOS* steady-state message levels, we hypothesized that transcriptional regulation of human *iNOS* may be regulated by distinct molecular mechanisms in a tissue-specific manner.

The cytokine-responsive *cis*-acting elements of the human *iNOS* promoter are contained within 16 kb of the start of transcription (7). To identify potential regulatory regions within this large 5′-flanking sequence, we analyzed this region for changes in chromatin structure in control and cytokine-stimulated cells. DNase I-HS sites may be used to map areas of chromatin functionally associated with *trans*-acting factors involved in the transcriptional regulation of a gene. To digest intact chromatin, we made cells permeable to DNase I with lysophosphatidylcholine. Pfeifer and Riggs (31) showed that cells permeabilized with lysophosphatidylcholine display in vivo DNase I footprints that are lost in samples from isolated nuclei; thus this method may preserve DNA-protein interactions that are disrupted by nuclear isolation methods. Shown in Fig. 2*A* are the restriction fragments

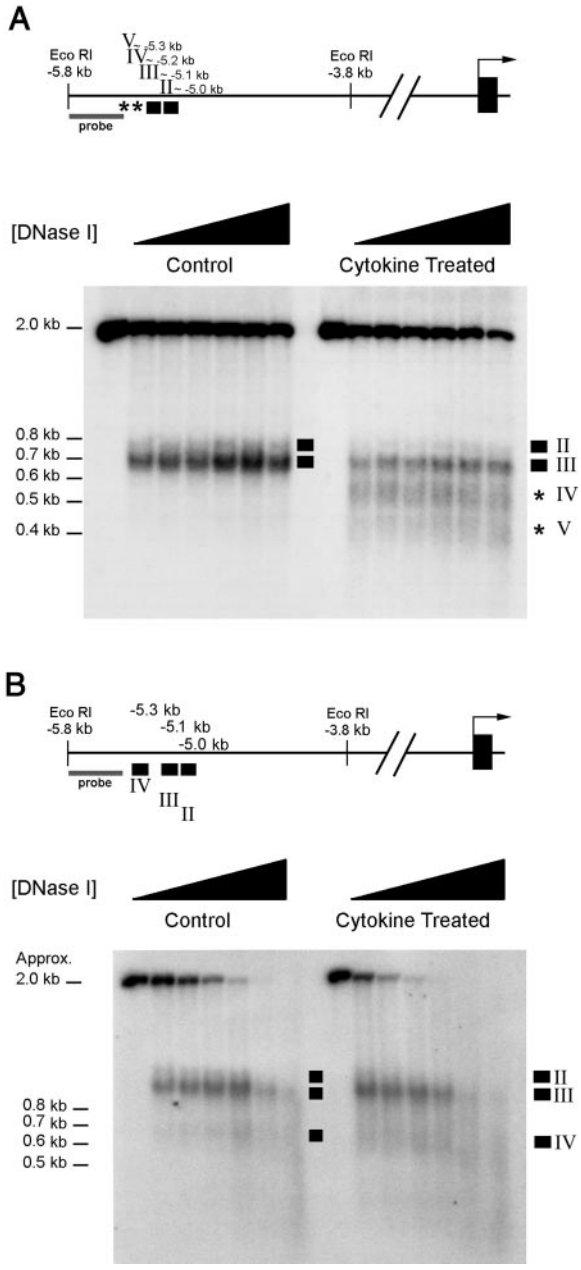

Fig. 3. Chromatin structure analysis of *region 3* in A549 (*A*) and AKN-1 (*B*) cells. Cell treatment and Southern analysis were performed as described in Fig. 2. The hybridization probe abutted the *Eco*RI site at −5.8 kb, detecting a 2.0-kb genomic restriction fragment. Two inducible (*) and two constitutive HS sites (solid boxes) mapped to this region in the A549 cells. A similar analysis in AKN-1 cells revealed only 3 constitutive HS sites.

and hybridization probes used in the chromatin structure analysis. The region analyzed was ~16 kb and included the first exon and intron and 13 kb of the 5′-flanking region.

Figure 2, *B* and *C*, shows a representative chromatin structure analysis of *region 1* in A549 and AKN-1 cells, respectively. We defined *region 1* by an *Eco*RI fragment from −3.8 to +2.3 kb that mediated only basal transcriptional activity based on promoter deletion analysis in AKN-1 cells (7). In control A549 samples (Fig.

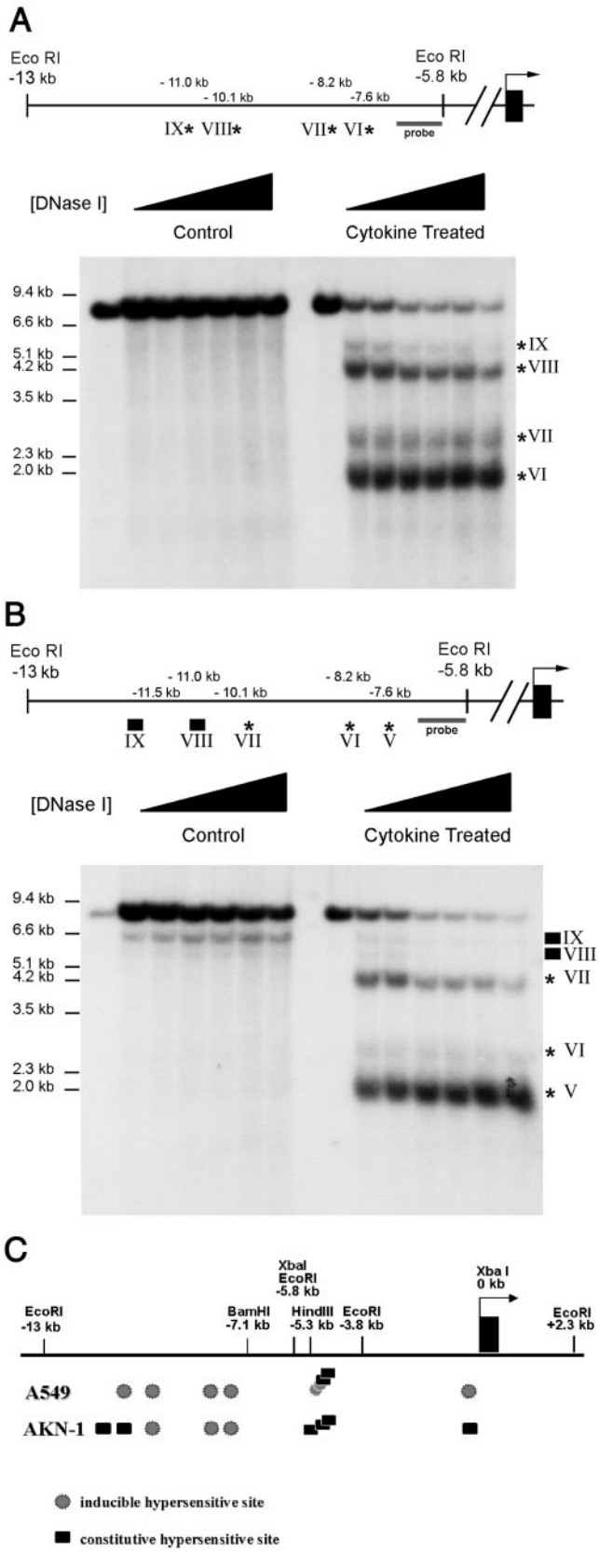

2*B*), the probe hybridized only to the large intact restriction fragment; however, in cytokine-treated samples, an additional DNase I-cleaved fragment appeard. In contrast, AKN-1 cells (Fig. 2*C*) demonstrated one constitutive DNase I-cleaved fragment in both control and treated cells. In both A549 and AKN-1 cells, this HS site mapped near the transcription initiation site. Although there was essentially no DNase I digestion of the control samples (see Fig. 2*B*), DNase I digestion was documented in these and all samples by ethidium bromide staining of size-fractionated DNA before restriction enzyme digestion.

An analysis of *region 2*, which mapped from −5.8 kb to +110 bp, shows a single DNase I-cleaved fragment in both control and cytokine-treated A549 and AKN-1 cells (data not shown). Because this DNase I-cleaved fragment migrated just slightly below the intact restriction fragment on a 0.8% high gelling temperature agarose gel, we employed a high-resolution analysis on a smaller restriction fragment contained within *region 2* to more clearly observe the DNase I cleavage pattern in this area. Figure 3 shows the analysis of *region 3*, defined by an *Eco*RI fragment that maps from −5.8 to −3.8 kb. These samples were size fractionated on NuSieve 3:1 agarose, which finely resolves DNA fragments < 2 kb in size. In both control and cytokine-treated A549 cells (Fig. 3*A*) digested with DNase I, two constitutive HS sites as well as two additional cytokine-specific HS sites were revealed. The chromatin structure of this region in the AKN-1 cells (Fig. 3*B*) revealed only three constitutive HS sites. An analysis of the chromatin structure in *region 4* (defined by a *Bam*HI-*Eco*RI fragment that maps from −7.1 to −5.8 kb) revealed no detectable DNase I-HS sites in either cell type (data not shown).

Figure 4 is a chromatin structure analysis of *region 5* evaluated with an *Eco*RI fragment extending from −13 to −5.8 kb. This fragment contained all but the upstream 3 kb of the 5′-flanking region shown to have a 10-fold transcriptional induction with cytokines in AKN-1 cells (7). In control A549 cells digested with DNase I (Fig. 4*A*), no HS sites were found; however, on stimulation with cytokines, four inducible DNase I HS sites appeared. In contrast, control AKN-1 cells had two constitutive HS sites (Fig. 4*B*), and cytokine-treated AKN-1 cells showed an additional three cytokine-inducible HS sites.

Figure 4*C* is a summary of the chromatin structure changes found in the 5′-flanking region of human *iNOS* in both control and cytokine-treated A549 and AKN-1 cells. The promoter had constitutive HS sites in both

Fig. 4. Chromatin structure analysis of *region 5*. Cell treatment and Southern analysis were performed as described in Fig. 2. DNase I-HS sites were detected with a probe that hybridized to a sequence 5′ to the *Eco*RI site at −5.8 kb, revealing the *Eco*RI fragment from −13 to −5.8 kb. *A*: this analysis revealed 4 cytokine-induced HS sites (*) in the A549 cells. *B*: in the AKN-1 cells, a similar analysis detected 2 constitutive (solid boxes) and 3 inducible (*) HS sites. *C*: summary of the chromatin structure analysis in the A549 and AKN-1 cells.

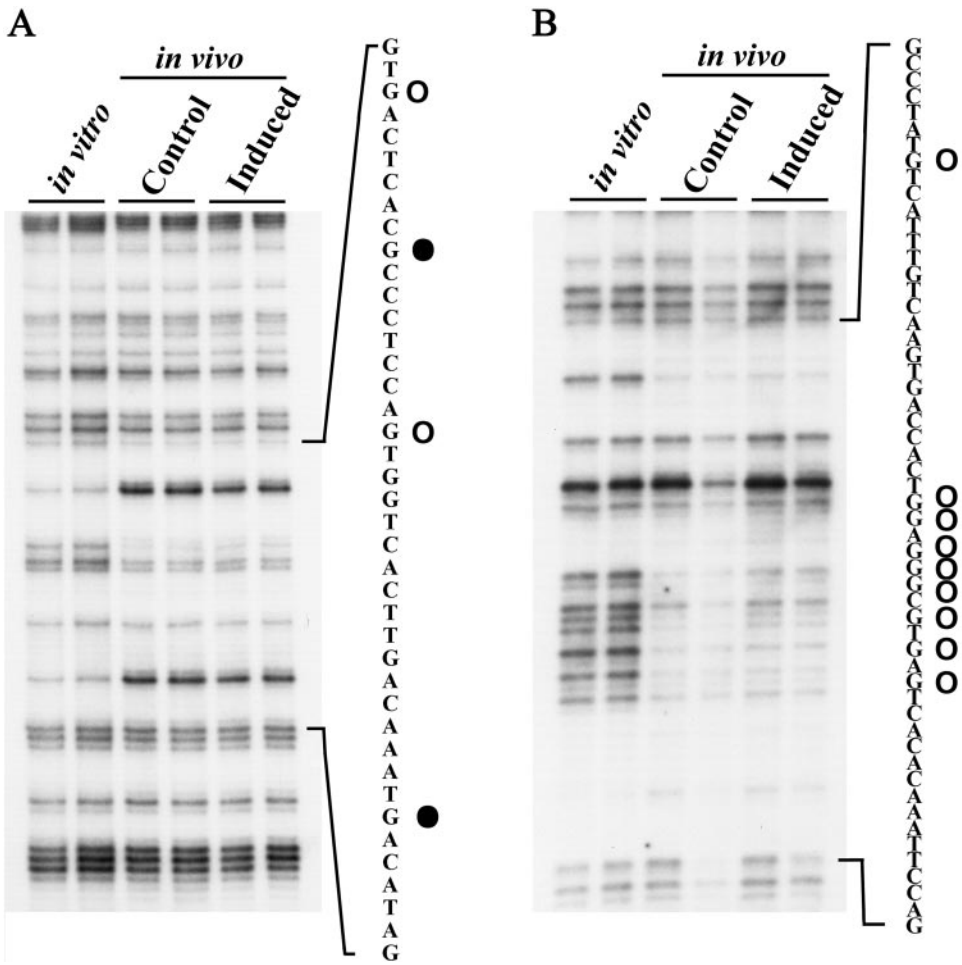

Fig. 5. In vivo dimethyl sulfate (DMS) footprinting: analysis of DNA-protein interactions in *region 3*. A549 cells were treated with DMS as described in EXPERIMENTAL PROCEDURES. *A*: primers used for ligation-mediated (LM) PCR analysis of the top strand were 5′-CAAATGATAAAGGTGGG-3′, 5′-GACGTGAAGGAAACACAGGGGCGTGG-3′, and the common linker primer 5′-GCGGTGACCCGGGAGATCTGAATTC-3′. After LMPCR and denaturing gel electrophoresis, sequence was displayed by hybridization with a strand-specific radiolabeled oligonucleotide probe, 5′-TGCATGTCCCGTGGCGAGTCACG-3′. *Lanes 1* and *2* were derived from protein-free DNA modified in vitro with DMS and served as controls to show each guanine residue. *Lanes 3–6* were derived from cells modified in vivo with DMS. Control, unstimulated cells; induced, cytokine-treated cells. *Right*, sequence of the bracketed area. ●, Enhancements; ○, protections. The basal footprints mapped within the constitutive DNase I-HS sites in *region 3* of both the A549 and AKN-1 cells. Identical in vivo footprinting results were obtained in AKN-1 cells. *B*: identical in vivo footprint analysis of the bottom strand was performed as described in *A* by using the LMPCR primers 5′-ATCCTGGAGTGACCACCG-3′ and 5′-TCCGTCATCTCCGAGTCAGGCAAGG-3′. The DNA sequence was displayed with the radiolabeled oligonucleotide probe 5′-AAGGTGGTGGAAACCGGGGAAGACC-3′. *Right*, constitutive in vivo contacts of the bracketed area.

cells lines; however, the induction of *iNOS* with cytokines was accompanied by dramatic changes in chromatin structure as revealed by the appearance of several inducible HS sites. Although most sites were shared between the two cell lines, each also had unique, tissue-specific sites.

To begin to localize specific DNA binding sites of *trans*-acting factors, we used DMS in vivo footprinting with LMPCR to analyze *region 3* in the vicinity of the HS sites. We chose this region because it contained both constitutive, inducible, and tissue-specific HS sites and because a genomic DNA sequence was available. Figure 5*A* shows in vivo footprinting on the top strand of constitutive HS *sites II* and *III* (Fig. 3) in A549 cells. Identical results were obtained in AKN-1 cells (data not shown). Enhanced DMS reactivity is seen at two guanine residues at −5,106 and −5,081 bp relative to the start of transcription. Additionally, two protected guanine residues are located at −5,113 and −5,098 bp. The results of in vivo footprinting on the bottom strand of this region are seen in Fig. 5*B*. A cluster of protections is seen at −5,111, −5,109, −5,107, −5,105, −5,104, −5,103, −5,101, and −5,100 bp. Additionally, an isolated protected guanine at −5,079 bp also shows decreased DMS reactivity. All of these constitutive in vivo footprints map to the HS *sites II* and *III* depicted in Fig. 3.

We also analyzed the inducible HS *sites IV* and *V* in *region 3* (Fig. 3*A*) by in vivo footprinting. In the A549 cells, the chromatin structure in this region contains cytokine-inducible HS *sites IV* and *V*; however, this region of chromatin is constitutively accessible in the AKN-1 cells (HS *site IV*). The results of in vivo footprinting on the top strand in A549 cells revealed enhanced DMS reactivity at −5,502 and −5,490 bp only in the samples prepared from cells treated with cytokines (Fig. 6). Interestingly, this cytokine-inducible footprint is seen in a constitutively accessible region of the chromatin in the AKN-1 cells. DMS footprint analysis of the bottom strand of this region showed no differential DMS reactivity (data not shown). Figure 7 summarizes the results of in vivo footprinting and the location of the DNase I-HS sites in *region 3*.

DISCUSSION

The physiological and pathophysiological roles of NO· can be placed into the three broad categories of neurotransmission, vasodilation, and inflammation, although its specific function in human diseases is

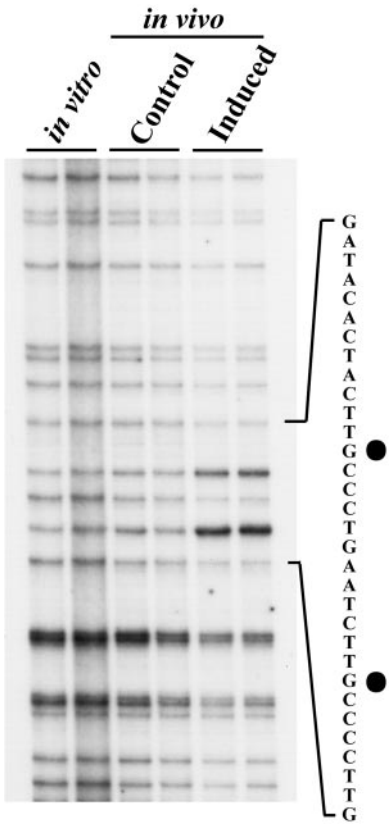

Fig. 6. In vivo DMS footprinting: identification of inducible DNA-protein interactions in *region 3*. Cells and DNA were prepared as described in Fig. 5. Top strand sequence 5′ to the constitutive in vivo DMS footprints in Fig. 5 was analyzed with LMPCR primers 5′-ACAAATTCCAGCAGCTCC-3′ and 5′-GTCTTCCCCGGTTTCCACC-ACCTTGC-3′. The sequence was displayed after hybridization with a radiolabeled oligonucleotide probe, 5′-GCCTGACTCGGAGAT-GACGG-3′. *Right*, sequence of the bracketed area. In this case, the enhanced hybridization signals (●) are seen only in the cytokine-treated samples. These cytokine-inducible footprints mapped near the region of the inducible DNase I-HS sites found in the A549 cells. Identical cytokine-induced enhancements were detected in AKN-1 cells, and interestingly, these inducible contacts were associated with the region of chromatin that was constitutively open in the AKN-1 cells, implying that a different mechanism was maintaining the open chromatin structure in these cells.

incompletely understood (19). NO· produced by *iNOS* is generated predominantly in settings of inflammation and infection and is elevated in many disease states such as asthma (1, 13, 14) and acute hepatic injury (15, 18, 35). iNOS expression is therefore coordinately upregulated with many other cytokine-induced genes such as manganese superoxide dismutase (38). Human *iNOS* is tightly regulated at the level of transcription, and multiple cytokines are required for maximal induction of steady-state mRNA levels, potentially implicating a complex array of *trans*-acting factors that mediate cytokine responsiveness. Adding to the complexity of the regulatory machinery, cells originating from different tissues have dissimilar requirements for cytokines to generate maximal induction, and the same cells from different species respond to dissimilar stimuli. It is perhaps not surprising, therefore, that sequences of human *iNOS* dispersed over 16 kb, as defined by promoter deletion analysis, confer 10-fold cytokine inducibility to a reporter gene. There is also a lack of cytokine-inducible activity in the proximal promoter as reported by de Vera et al. (7) and Linn et al. (23) in deletion analysis in liver and colonic epithelial cells, respectively. Our chromatin structure analysis of the first 3.8 kb of the 5′-flanking region, which identified a single constitutive HS site located at the transcription start site, supports the lack of cytokine-inducible regulatory elements in the proximal promoter in AKN-1 cells. This HS site is cytokine inducible in the A549 cells, however, and binding of factors to this region may account for the threefold cytokine inducibility reported by Nunokawa et al. (27) in these cells.

Overall, our chromatin structure analysis corroborates the promoter deletion data reported by de Vera et al. (7). In their analysis, however, the reporter gene construct that contained 7.1 kb of promoter sequence conferred additional cytokine inducibility compared with the construct that contained only 5.8 kb. When we examined the sequence between −5.8 and −7.1 kb for DNase I-HS sites, none were found. To address whether any HS sites located very close to the ends of the restriction fragment may not have been resolved, we repeated the analysis of this region with a *Bam*HI-*Hin*dIII restriction fragment that maps from −7.1 to −5.3 kb and an *Eco*RI fragment that maps from −5.8 to −13 kb, with the same result. The transcriptional activity found with sequences out to −7.1 kb may be a consequence of the inability of a plasmid-based construct to attain a chromatin structure resembling that of the endogenous gene. Thus the role that chromatin structure normally plays in transcriptional repression would not have been seen, and this region could be functionally active in this in vitro promoter deletion assay. An analogous situation was uncovered in the case of the β-phaseolin (*phas*) gene (21). In these studies, tobacco plants stably transformed with constructs of the *phas* promoter and the lethal diphtheria toxin A-chain reporter gene developed normally until *phas* activation in the heart stage of embryogenesis that resulted in death. In contrast, similar constructs containing the nonlethal *uidA* reporter transiently transfected by bombardment or electroporation showed abundant transcription. Thus the same promoter sequence when ligated into the chromatin was regulated in a radically different manner than when transiently transfected. A similar scenario could explain the additional cytokine-inducible promoter activity displayed by the region of the human *iNOS* promoter that does not demonstrate open chromatin regions defined by DNase I-HS sites.

When de Vera et al. (7) tested 16 kb of the human *iNOS* promoter in a reporter gene construct, they attained a 10-fold induction of reporter gene activity on cytokine treatment of the AKN-1 cells. When we examined sequences between −5.8 and −13 kb, we found dramatic changes in the chromatin structure in both the A549 and the AKN-1 cell lines, changes that were reminiscent of those seen in the chicken lysozyme gene (9). This promoter region in the AKN-1 cells contained

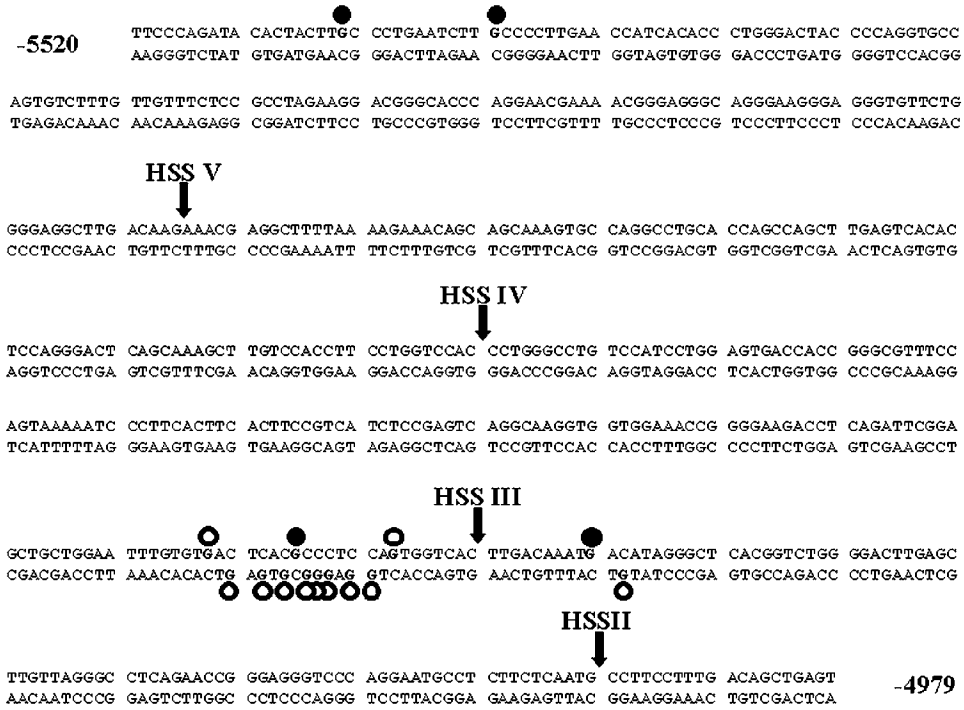

Fig. 7. Summary of DNase I-HS site (HSS) analysis and in vivo DMS footprint results in *region 3*. Shown is the sequence from −5,520 to −4,979 kb of the human *iNOS* promoter, summarizing the cytokine-inducible and constitutive in vivo footprints in A549 and AKN-1 cells relative to the DNase I-HS sites mapped in the A549 cells (HS *sites II–IV*). ●, Enhancements; ○, protections. Arrows, approximate midpoints of the DNase I-HS sites.

constitutive, cytokine-inducible, and unique tissue-specific HS sites. This same region of the promoter in A549 cells contained only cytokine-inducible HS sites.

When the results of the chromatin structure data are examined as a whole, interesting details emerge. Although many of the DNase I-HS sites map to the same promoter regions in both cell lines, the HS sites are more likely to be constitutive in the AKN-1 cells and inducible in the A549 cells. These chromatin structure differences may reflect the different requirements that the cytokines required to minimally induce the *iNOS* steady-state message levels. Many of the HS sites in the AKN-1 cells are constitutively accessible and thus presumably already bound by transcription factors, and these cells require only the single cytokine IFN-γ. Regulation of transcription in A549 cells is more involved, requiring both IFN-γ and IL-1β to minimally induce the message. Cytokine induction in these cells is therefore accompanied by additional changes in the chromatin structure. In addition, the two cell lines also have unique, tissue-specific HS sites reflecting the tissue-specific regulation of *iNOS*.

Promoter deletion studies implicate sequences up to 16 kb upstream from the transcription start site in the cytokine-inducible transcriptional regulation of *iNOS* (7), whereas our chromatin structure analysis successfully narrowed the promoter regions in which to search for functional elements. Using DNase I-HS sites as a guide, we used in vivo footprinting with LMPCR to examine one functionally relevant area at single-nucleotide resolution for sequence-specific DNA-protein interactions.

Based on the availability of sequence data and the presence of constitutive, cytokine-inducible, and tissue-specific HS sites, we chose to analyze the HS sites in *region 3* from approximately −5.45 to −4.95 kb. We found a good correlation between the functional role of the promoter region analyzed, the conformation of its chromatin, and the nature of the in vivo footprints. The promoter deletion analysis identified *region 3* (downstream from −5.8 kb) as conferring a modest threefold increase in reporter gene activity on stimulation with cytokines in the AKN-1 cells, and the inducible footprints map to the location of the inducible HS *sites IV* and *V* in the A549 cells (Fig. 3). Thus the binding of a cytokine-inducible *trans*-acting factor(s) likely causes the cytokine-inducible DMS footprints. Additionally, the constitutive footprints map within an area of chromatin that is constitutively accessible in both cell lines. Interestingly, the inducible footprints bind within an area of constitutively accessible chromatin in the AKN-1 cells. This may be related to the transcriptional mechanism that allows a single cytokine to minimally stimulate the *iNOS* steady-state message levels, whereas the A549 cells require two cytokines for minimal induction.

A computer analysis of the sequence surrounding the inducible and constitutive footprints identified numerous putative consensus sequences. Only the growth factor independence (*Gfi-1*) transcription factor consensus sequence significantly overlapped the inducible DMS footprints. However, we have ruled out involvement of *Gfi-1* in the transcriptional regulation of human *iNOS* based on its limited tissue distribution in adult animals (10, 41). Independently, Taylor et al. (36) have used computer sequence analysis to identify putative nuclear factor-κB binding sites within 7 kb of the transcription initiation site. Mutated nuclear factor-κB sites evaluated by transient transfection studies implied that specific elements located within the region

we analyzed by in vivo footprinting affected reporter gene activity. Our in vivo footprinting data do not show any evidence of differential DMS reactivity at these sites in this region. Therefore, our inducible DMS footprints are likely caused by the binding of a cytokine-inducible, previously undescribed sequence-specific DNA binding protein.

Based on the number of nucleotides that separate them, the footprints located from −5,113 to −5,098 bp define constitutive binding *site I*, and the enhancement at −5,081 bp and the protection at −5,079 bp define binding *site II*. Computer analysis identified activator protein (AP)-1 and Ets-1 consensus sequences within two palindromes that span binding *site I*. The Ets-1 consensus sequence in binding site I contains the invariant GGA, shown to be critical for DNA binding activity by methylation interference analysis (30). As seen in constitutive binding *site I*, not only the invariant GGA but also every G residue in the putative Ets-1 consensus sequence is protected in vivo.

In addition to the footprints in the Ets-1 consensus sequence, top and bottom strand guanine residues in the AP-1 consensus sequence are also protected, possibly indicating that these residues are also involved in DNA binding of an AP-1-Ets-1 heterotrimer. Another study (2) has shown that the Ets-1 and AP-1 transcription factors can interact to form a heterotrimer. For example, this heterotrimeric complex forms on the granulocyte-macrophage colony-stimulating factor promoter as shown by Thomas et al. (37). The arrangement of the AP-1 and Ets-1 consensus sequences on this promoter is very similar to that seen in binding site I. Specifically, the AP-1 and Ets-1 consensus sequences are in very close proximity with the Ets-1 sequence positioned on the bottom strand. Binding *site II* also overlaps a palindrome that contains an AP-1 consensus sequence. The footprint pattern in this AP-1 consensus sequence is different from that seen in binding *site I*. Formation of an AP-1-Ets-1 heterotrimer may affect the interaction of AP-1 with its consensus sequence, thus affecting DMS reactivity of the guanine residues. The only caveat to the potential involvement of AP-1 is its almost exclusive distinction as an inducible factor. Based on recent evidence, however, constitutive AP-1 binding has been shown in some unstimulated cells (4).

Based on computer analysis, Marks-Konczalik et al. (25) mutated, among others, putative AP-1 sites at −5,115 and −5,301 bp and found a decrease in reporter gene activity. The AP-1 consensus sequence at −5,115 bp is identical to the AP-1 sequence found in our footprinted binding site I. However, we found no evidence for binding of the consensus sequence at −5,301 bp. A potential explanation for the differences between our in vivo footprinting data and results from transient transfection studies is the inability of plasmid constructs to reduplicate the in vivo chromatin structure of the endogenous gene.

In conclusion, we have shown direct evidence that human *iNOS* is regulated by cytokines in a tissue-specific manner. Furthermore, we have identified DNA-protein interactions in AP-1 and Ets-1 binding sites within a region of the promoter known to play a functional role in the transcriptional regulation of this gene. We have also identified a novel, previously undescribed, cytokine-inducible in vivo DNA footprint.

This work was supported by grants from the American Lung Association of Florida (to S. E. Chesrown).

REFERENCES

1. **Barnes PJ.** Nitric oxide and asthma. *Res Immunol* 146: 698–702, 1995.
2. **Basuyaux JP, Ferreira E, Stehelin D, and Buttice GJ.** The Ets transcription factors interact with each other and with the c-Fos/c-Jun complex via distinct domains in a DNA-dependent and -independent manner. *J Biol Chem* 272: 26188–26195, 1997.
3. **Blackford JA Jr, Antonini JM, Castranova V, and Dey RD.** Intratracheal instillation of silica up-regulates inducible nitric oxide synthase gene expression and increases nitric oxide production in alveolar macrophages and neutrophils. *Am J Respir Cell Mol Biol* 11: 426–431, 1994.
4. **Botelho FM, Edwards DR, and Richards CD.** Oncostatin M stimulates c-Fos to bind a transcriptionally responsive AP-1 element within the tissue inhibitor of metalloproteinase-1 promoter. *J Biol Chem* 273: 5211–5218, 1998.
5. **Charles IG, Palmer RM, Hickery MS, Bayliss MT, Chubb AP, Hall VS, Moss DW, and Moncada S.** Cloning, characterization and expression of a cDNA encoding an inducible nitric oxide synthase from the human chondrocyte. *Proc Natl Acad Sci USA* 90: 11419–11423, 1993.
6. **Del Pozo V, de Arruda-Chaves E, de Andres B, Cardaba B, Lopez-Farre A, Gallardo S, Cortegano I, Vidarte L, Jurado A, Sastre J, Palomino P, and Lahoz CJ.** Eosinophils transcribe and translate messenger RNA for inducible nitric oxide synthase. *Immunology* 158: 859–864, 1997.
7. **De Vera ME, Shapiro RA, Nussler AK, Mudgett JS, Simmons RL, Morris SM Jr, Billiar TR, and Geller DA.** Transcriptional regulation of human inducible nitric oxide synthase (NOS2) gene by cytokines: initial analysis of the human NOS2 promoter. *Proc Natl Acad Sci USA* 93: 1054–1059, 1996.
8. **Evans CH.** Nitric oxide: what role does it play in inflammation and tissue destruction? *Agents Actions Suppl* 47: 107–116, 1995.
9. **Fritton HP, Igo-Kemenes T, Nowock J, Strech-Jurk U, Theisen M, and Sippel AE.** Alternative sets of DNase I-hypersensitive sites characterize the various functional states of the chicken lysozyme gene. *Nature* 311: 163–165, 1984.
10. **Fuchs B, Wagner T, Rossel N, Antoine M, Beug H, and Niessing J.** Structure and erythroid cell-restricted expression of a chicken cDNA encoding a novel zinc finger protein of the Cys + His class. *Gene* 195: 277–284, 1997.
11. **Geller DA, Lowenstein CJ, Shapiro RA, Nussler AK, Di Silvio M, Wang SC, Nakayama DK, Simmons RL, Snyder SH, and Billiar TR.** Molecular cloning and expression of inducible nitric oxide synthase from human hepatocytes. *Proc Natl Acad Sci USA* 90: 3491–3495, 1993.
12. **Gross DS and Garrard WT.** Nuclease hypersensitive sites in chromatin. *Annu Rev Biochem* 57: 159–197, 1988.
13. **Guo FH, Comhair SAA, Zheng S, Dweik RA, Eissa NT, Thomassen MJ, Calhoun W, and Erzurum SC.** Molecular mechanisms of increased nitric oxide (NO) in asthma: evidence for transcriptional and post-translational regulation of NO synthesis. *J Immunol* 164: 5970–5980, 2000.
14. **Hamid Q, Springall DR, Riveros-Moreno V, Chanez P, Howarth P, Redington A, Bousquet J, Godard P, Holgate S, and Polak JM.** Induction of nitric oxide synthase in asthma. *Lancet* 342: 1510–1513, 1993.
15. **Hangai M, Yoshimura N, Hiroi K, Mandai M, and Honda Y.** Inducible nitric oxide synthase in retinal ischemia-reperfusion injury. *Exp Eye Res* 63: 501–509, 1996.
16. **Hierholzer C, Harbrecht B, Menezes JM, Kane J, MacMicking J, Nathan CF, Peitzman AB, Billiar TR, and**

Tweardy DJ. Essential role of induced nitric oxide in the initiation of the inflammatory response after hemorrhagic shock. *J Exp Med* 187: 917–928, 1998.

17. **Hornstra IK and Yang TP.** In vivo footprinting and genomic sequencing by ligation-mediated PCR. *Anal Biochem* 213: 179–193, 1993.
18. **Koda W, Harada K, Tsuneyama K, Kono N, Sasaki M, Matsui O, and Nakanuma Y.** Evidence of the participation of peribiliary mast cells in regulation of the peribiliary vascular plexus along the intrahepatic biliary tree. *Lab Invest* 80: 1007–1017, 2000.
19. **Kroncke KD, Fehsel K, and Kolb-Bachofen V.** Inducible nitric oxide synthase in human diseases. *Clin Exp Immunol* 113: 147–156, 1998.

19a. **Kuo S, Chesrown SE, Mellott JK, Rogers RJ, Hsu IL, and Nick H.** In vivo architecture of the manganese superoxide dismutase promoter. *J Biol Chem* 274: 3345–3354, 1999.

20. **Laubach VE, Zhang CX, Russell SW, Murphy WJ, and Sherman PA.** Analysis of expression and promoter function of the human inducible nitric oxide synthase gene in DLD-1 cells and monkey hepatocytes. *Biochim Biophys Acta* 1351: 287–295, 1997.
21. **Li G, Chandler SP, Wolffe AP, and Hall TC.** Architectural specificity in chromatin structure at the TATA box in vivo: nucleosome displacement upon beta-phaseolin gene activation. *Proc Natl Acad Sci USA* 95: 4772–4777, 1998.
22. **Lieber M, Smith B, Szakal A, Nelson-Rees W, and Todaro G.** A continuous tumor-cell line from a human lung carcinoma with properties of type II alveolar epithelial cells. *Int J Cancer* 17: 62–70, 1976.
23. **Linn SC, Morelli PJ, Edry I, Cottongim SE, Szabo C, and Salzman AL.** Transcriptional regulation of human inducible nitric oxide synthase gene in an intestinal epithelial cell line. *Am J Physiol Gastrointest Liver Physiol* 272: G1499–G1508, 1997.
24. **Majano PL, Garcia-Monzon C, Lopez-Cabrera M, Lara-Pezzi E, Fernandez-Ruiz E, Garcia-Iglesiase C, Borque MJ, and Moreno-Otero R.** Inducible nitric oxide synthase expression in chronic viral hepatitis. Evidence for a virus-induced gene upregulation. *J Clin Invest* 101: 1343–1352, 1998.
25. **Marks-Konczalik J, Chu SC, and Moss J.** Cytokine-mediated transcriptional induction of the human inducible nitric oxide synthase gene requires both activator protein 1 and nuclear factor kappaB-binding sites. *J Biol Chem* 273: 22201–22208, 1998.
26. **Morris SM Jr and Billiar TR.** New insights into the regulation of inducible nitric oxide synthesis. *Am J Physiol Endocrinol Metab* 266: E829–E839, 1994.
27. **Nunokawa Y, Oikawa S, and Tanaka S.** Expression of human inducible nitric oxide synthase is regulated by both promoter and 3′-regions. *Biochem Biophys Res Commun* 233: 523–526, 1997.
28. **Nussler AK and Billiar TR.** Inflammation, immunoregulation, and inducible nitric oxide synthase. *J Leukoc Biol* 54: 171–178, 1993.
29. **Nussler AK, Vergani G, Gollin SM, Dorko K, Gansauge S, Morris SM Jr, Demetris AJ, Nomoto M, Beger HG, and Strom SC.** Isolation and characterization of a human hepatic epithelial-like cell line (AKN-1) from a normal liver. *In Vitro Cell Dev Biol Anim* 35: 190–197, 1999.
30. **Nye JA, Petersen JM, Gunther CV, Jonsen MD, and Graves BJ.** Interaction of murine ets-1 with GGA-binding sites establishes the ETS domain as a new DNA-binding motif. *Genes Dev* 6: 975–990, 1992.
31. **Pfeifer GP and Riggs AD.** Chromatin differences between active and inactive X chromosomes revealed by genomic footprinting of permeabilized cells using DNase I and ligation-mediated PCR. *Genes Dev* 5: 1102–1113, 1991.
32. **Robbins RA, Barnes PJ, Springall DR, Warren JB, Kwon OJ, Buttery LD, Wilson AJ, Geller DA, and Polak JM.** Expression of inducible nitric oxide in human lung epithelial cells. *Biochem Biophys Res Commun* 203: 209–218, 1994.
33. **Salzman AL.** Nitric oxide in the gut. *New Horiz* 3: 352–364, 1995.
34. **Spitsin SV, Koprowski H, and Michaels FH.** Characterization and functional analysis of the human inducible nitric oxide synthase gene promoter. *Mol Med* 2: 226–235, 1996.
35. **Taylor BS, Alarcon LH, and Billiar TR.** Inducible nitric oxide synthase in the liver: regulation and function. *Biochemistry (Mosc)* 63: 766–781, 1998.
36. **Taylor BS, de Vera ME, Ganster RW, Wang Q, Shapiro RA, Morris SM Jr, Billiar TR, and Geller DA.** Multiple NF-kappaB enhancer elements regulate cytokine induction of the human inducible nitric oxide synthase gene. *J Biol Chem* 273: 15148–15156, 1998.
37. **Thomas RS, Tymms MJ, McKinlay LH, Shannon MF, Seth A, and Kola I.** ETS1, NFkappaB and AP1 synergistically transactivate the human GM-CSF promoter. *Oncogene* 14: 2845–2855, 1997.
38. **Visner GA, Dougall WC, Wilson JM, Burr IA, and Nick HS.** Regulation of manganese superoxide dismutase by lipopolysaccharide, interleukin-1, and tumor necrosis factor. Role in the acute inflammatory response. *J Biol Chem* 265: 2856–2864, 1990.
39. **Worrall NK, Boasquevisque CH, Misko TP, Sullivan PM, Ferguson TB Jr, and Patterson GA.** Inducible nitric oxide synthase is expressed during experimental acute lung allograft rejection. *J Heart Lung Transplant* 16: 334–339, 1997.
40. **Yun HY, Dawson VL, and Dawson TM.** Nitric oxide in health and disease of the nervous system. *Mol Psychiatry* 2: 300–310, 1997.
41. **Zweidler-Mckay PA, Grimes HL, Flubacher MM, and Tsichlis PN.** Gfi-1 encodes a nuclear zinc finger protein that binds DNA and functions as a transcriptional repressor. *Mol Cell Biol* 16: 4024–4034, 1996.